Korean J. Chem. Eng., **31**(8), 1368-1376 (2014)
DOI: 10.1007/s11814-014-0053-z

pISSN: 0256-1115
eISSN: 1975-7220

Presulfidation and activation mechanism of Mo/Al_2O_3 catalyst sulfided by ammonium thiosulfate

Mingxing Tang, Hui Ge, Weibin Fan, Guofu Wang, Zhanjun Lyu, and Xuekuan Li†

State Key laboratory of Coal Conversion Institute of Coal Chemistry, Chinese Academy of Sciences, Taiyuan 030001, China
(*Received 12 October 2013 • accepted 10 February 2014*)

Abstract−Mo/Al_2O_3 catalyst was presulfided with $(NH_4)_2S_2O_3$ to elucidate presulfidation and activation mechanism. It is illustrated that the Mo oxide is firstly partially sulfided during presulfidation and then in situ reduced into MoS_{2-x} in activation, and finally sulfided to active state during hydrodesulfurization (HDS). A synergistic effect between the S^{2-} and S^{6+} ions in $(NH_4)_2S_2O_3$ produces a positive influence on the HDS performance. The S^{2-} ions contribute to the sulfidation of Mo ions, while the S^{6+} species interact with Al_2O_3 support, weakening the interaction of active species with support.

Keywords: Hydrodesulfurization, Ammonium Thiosulfate, Presulfidation, Activation, Support Interaction

INTRODUCTION

Mo-based hydrodesulfurization (HDS) catalysts have been used in industrial hydrotreating processes for decades [1]. Commercial HDS catalysts are usually available in an oxide form and must be activated by a gas or liquid sulfiding agent, such as H_2S, CS_2 or CH_3SSCH_3 (DMDS) [2-4]. However, the use of such malodorous and noxious compounds causes environmental pollution and is harmful to the operators. Presulfidation technologies, due to their environmentally friendly character and easy operation, have attracted much interest by refineries [5-7], where the oxide catalysts are presulfided in advance with a solution of elemental sulfur or polysulfide followed by heat-treatment, to partially convert the metal oxide to sulfides. Then, the partly sulfided catalyst is loaded into reactor for hydrogen activation. The catalytic activity of sulfided catalyst is strongly influenced by the nature of the sulfiding agent and the activation conditions [8,9].

The in situ sulfidation of HDS catalysts by gas or liquid sulfiding agents has been extensively studied [10-16]. Unpromoted Mo/Al_2O_3 is often used as model catalyst to reveal the relations between active phase and HDS performance. With ESR, XPS and Raman spectroscopies, different intermediates such as oxysulfides and MoS_3 can be identified in various proportions during temperature-programmed sulfidation. But in final catalyst, the Mo is mainly present as MoS_2; however, the morphology and structure of MoS_2 may be considerably different, depending on the state of the oxide precursor, the sulfiding agent, and the temperature and duration of sulfidation [17].

In alumina-supported (Co)Mo sulfide at least two type of phases were observed: single-layer type I phase is only partially sulfided owing to the strong Mo-O-Al linkages with the support; multi-layer type II phase can be fully sulfided due to a weak interaction with alumina [18], the type II phase shows an activity twice as that of the type I phase [19]. Dugulan et al. [20] found that $(Co)Mo/Al_2O_3$ sulfided at high-pressure shows much higher HDS activity than at 1 atm due to formation of Type II Co-Mo-S phase. DFT calculation reveals that the formation of Mo-O-Al linkages increases the energy to remove sulfur atoms from the active surface to form coordinatively unsaturated Mo sites (CUS), which is considered the active site of HDS [21]. The Mo-O-Al linkages are preferred to locate at the S edge in MoS_2 slabs. Both Mo and S edges may form CUS but with different catalytic properties [23]; the nature of exposed edges depends on the preparation and activation conditions [24].

The sulfiding conditions impose important effects on the morphology, dispersion and structures of MoS_2 slabs, and consequently HDS activity. An insight into the sulfidation and activation mechanism is beneficial to the application of presulfidation process. However, few studies have contributed to such a process. In previous work we found that Mo-based catalyst presulfided with $(NH_4)_2S_2O_3$ showed high sulfidation degree and HDS activity [25]. In this paper, we focus on the presulfidation and activation mechanism of $(NH_4)_2S_2O_3$.

EXPERIMENTAL

1. Catalyst Preparation

The γ-Al_2O_3 support was impregnated with a concentrated ammonium solution of $(NH_4)_6Mo_7O_{24}\cdot 4H_2O$ by the pore filling method. The impregnated sample was dried at 110 °C for 12 h and calcined at 450 °C for 4 h. The prepared Mo/Al_2O_3 catalyst contained 8 wt% Mo. The Mo/Al_2O_3 catalysts were presulfided by two methods: 1) Mo/Al_2O_3 catalysts calcined at 450 or 600 °C was impregnated with an aqueous solution of $(NH_4)_2S_2O_3$ by the pore filling method, and dried at 90 °C for 2 h. These obtained samples were denoted as MoS3-450 and MoS3-600, respectively. 2) The γ-Al_2O_3 support catalyst was co-impregnated with the ammonium solution of $(NH_4)_6Mo_7O_{24}\cdot 4H_2O$ and $(NH_4)_2S_2O_3$, and dried at 90 °C for 2 h; the obtained catalyst is designated as MoS3-dry. The Mo content of MoS3-dry catalysts was also 8 wt% after calcinations. The presulfided catalysts have an S/Mo molar ratio of 3.0.

2. Activation and HDS Activity of the Prepared Catalysts

The activation and the HDS test were carried out in a fix-bed micro reactor. The catalyst loading was 0.1 g (40-60 mesh), without includ-

†To whom correspondence should be addressed.
E-mail: lxk@sxicc.ac.cn

ing presulfiding agent and absorbed water. Presulfided catalyst was in situ activated under hydrogen. For presulfided catalyst, the system was heated from room temperature to 300 °C at a rate of 5 °C/min and a pressure of 3.0 MPa under a hydrogen flow of 33 mL/min. Then it was kept at 300 °C for 0.5 h, followed by cooling to the reaction temperature of 280 °C. For comparison, the Mo/Al_2O_3 catalyst was sulfided with a flow of DMDS solution (1.5 wt% DMDS in nonane, 0.08 mL/min) at 3.0 MPa flowing hydrogen (33 mL/min). The detailed procedures are as follows: The reactor was first heated to 200 °C, and then the sulfiding feed was introduced; the temperature was first kept for 2 h, followed by increasing from 200 to 350 °C at a rate of 2.5 °C/min; the sulfidation was then continued for 4 h; finally the reactor was cooled to reaction temperature.

The HDS of thiophene was performed at 280 °C in a H_2 flow (3.0 MPa, 33 mL/min). 1.5 wt% thiophene in nonane was pumped into the reactor at a liquid velocity of 0.08 mL/min. The product oil was collected in a liquid collector and measured on a Shimadzu GC-14B chromatograph packed with an OV-101 capillary column and equipped with an FID detector. The spent catalysts were washed with n-hexane solvent and sealed under Ar into glass bottle for characterizations.

3. Catalyst Characterization

High resolution transmission electron microscopic (HRTEM) images of the spent catalysts were obtained on a JEOL JEM-2010 microscope operated at 200 kV. For estimation of the stacking and size distribution of MoS_2 crystallites, more than 400 crystallites were measured. The average slab length and stacking degree were calculated according to following equation: $\overline{M}=\sum_{i=1}^{n} n_i M_i / \sum_{i=1}^{n} n_i$, where M_i is the slab length or number of slabs of a MoS_2 unit and n_i the number of slabs or stacks in a determined range of length or stacking number.

For the fresh catalysts, the total sulfur content was measured by chemical analysis [26]. The S^{2-} content of the spent catalyst was performed on a micro coulometer (KZDL-3, Hebi-gaoke, China) by coulomb titration method. The carbon content in spent catalyst was measured by combustion method [27].

The surface area and pore properties of the catalysts were measured by nitrogen adsorption at 77 K with a Tristar 3000 (Micromeritics Instrument Co., USA). Before analysis, the catalysts were degassed at 60 °C for dried samples or at 200 °C for other samples in a vacuum of 0.13 Pa for 6-8 h.

Thermogravimetry-mass spectrometer (TG-MS) tests were conducted on a Setaram TGA92 thermogravimetry instrument connected with an OmniStar 200 quadrupole mass spectrometer. The connecting pipes were heated at 200 °C to avoid deposition of effluents. In each run, ca. 30 mg catalyst was loaded, and the temperature was ramped from room temperature to 600 °C at a rate of 10 °C/min. The m/z signals of H_2 (2), H_2O (18), S (32), H_2S (34), SO_2 (64) and SO_3 (80) in effluents were recorded by mass spectrometer. The experiments on presulfided catalysts were conducted under reductive atmosphere (10%H_2-90%Ar). For comparison, a sample of $(NH_4)_2S_2O_3/Al_2O_3$ was prepared by impregnation of alumina support with the same amount of ammonium thiosulfate used in presulfided catalysts. This sample was measured under reductive gas and simulating air (21%O_2-79%Ar).

X-ray photoelectron spectra (XPS) were measured on a Physical Electronics Company Quantum-2000 Scanning ESCA Microprobe spectroscope (Al Kα). Each sample was loaded in a glovebox and transported into the instrument under N_2 protection. Binding energy (BE) was calibrated with signal of contaminated carbon at 284.6 eV.

The temperature programmed desorption of ammonia (NH_3-TPD) was performed using a quartz micro reactor TP-5000 (Tianjing-Xianquan, China). About 50 mg sample was loaded in each run. The sample was first pretreated in an Ar flow of 50 mL/min at 500 °C for 2 h, and then cooled to 120 °C. This was followed by pulse-injecting enough ammonia. Further, the sample was flushed with the Ar flow at 120 °C for 1 h to remove physically adsorbed ammonia. Finally, the temperature was raised from 120 to 500 °C at a rate of 10 °C/min. The amount of desorbed NH_3 was measured with a thermal coupled detector (TCD). The profiles of NH_3-TPD were deconvolved by Gaussian method.

RESULTS

1. Thiophene HDS Activity

Fig. 1 shows the conversion of thiophene vs. time on stream. At least 8-10 hours was needed for MoS3-dry and MoS3-450 to achieve stability. During this period, the thiophene HDS activity increased with the time on stream. This suggests that the catalysts might not be well sulfided during hydrogen activation. They were continually sulfided by thiophene during HDS reaction. At initial stage, the MoS3-450 showed higher thiophene conversion than MoS3-dry. However, after about 5 h, the MoS3-dry surpassed MoS3-450. Owing to no calcinations applied to the MoS3-dry, this catalyst was presented at wet status and was more difficult to be effectively sulfided. Contrarily, MoS3-600 and Mo/Al_2O_3 seem to have been sufficiently sulfided during activation. No apparent stabilized duration was observed. MoS3-600 was calcined at 600 °C before impregnation with ammonium thiosulfate. Although the high temperature calcination had negative effect on the HDS activity, the catalyst was easier to achieve stabilization. Because the Mo/Al_2O_3 was effectively sulfided by DMDS, the HDS activity maintained stable during the test.

It is clear that the HDS activities of presulfided catalysts were

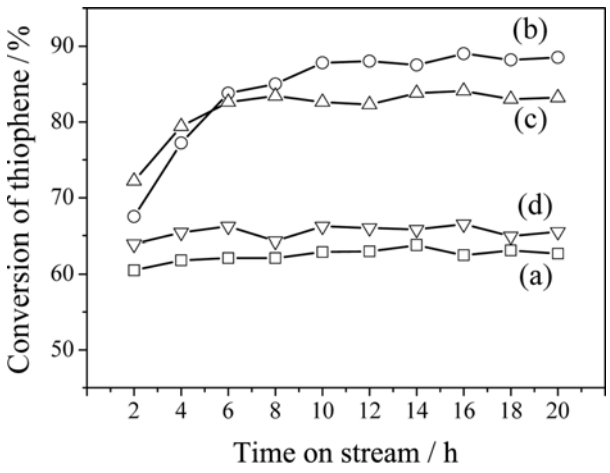

Fig. 1. Thiophene conversion vs. time on stream over (a) Mo/Al_2O_3, (b) MoS3-dry, (c) MoS3-450, (d) MoS3-600. Reaction conditions: 3.0 MPa, V(H_2)/V(oil)=412, LHSV=4.0 h^{-1}.

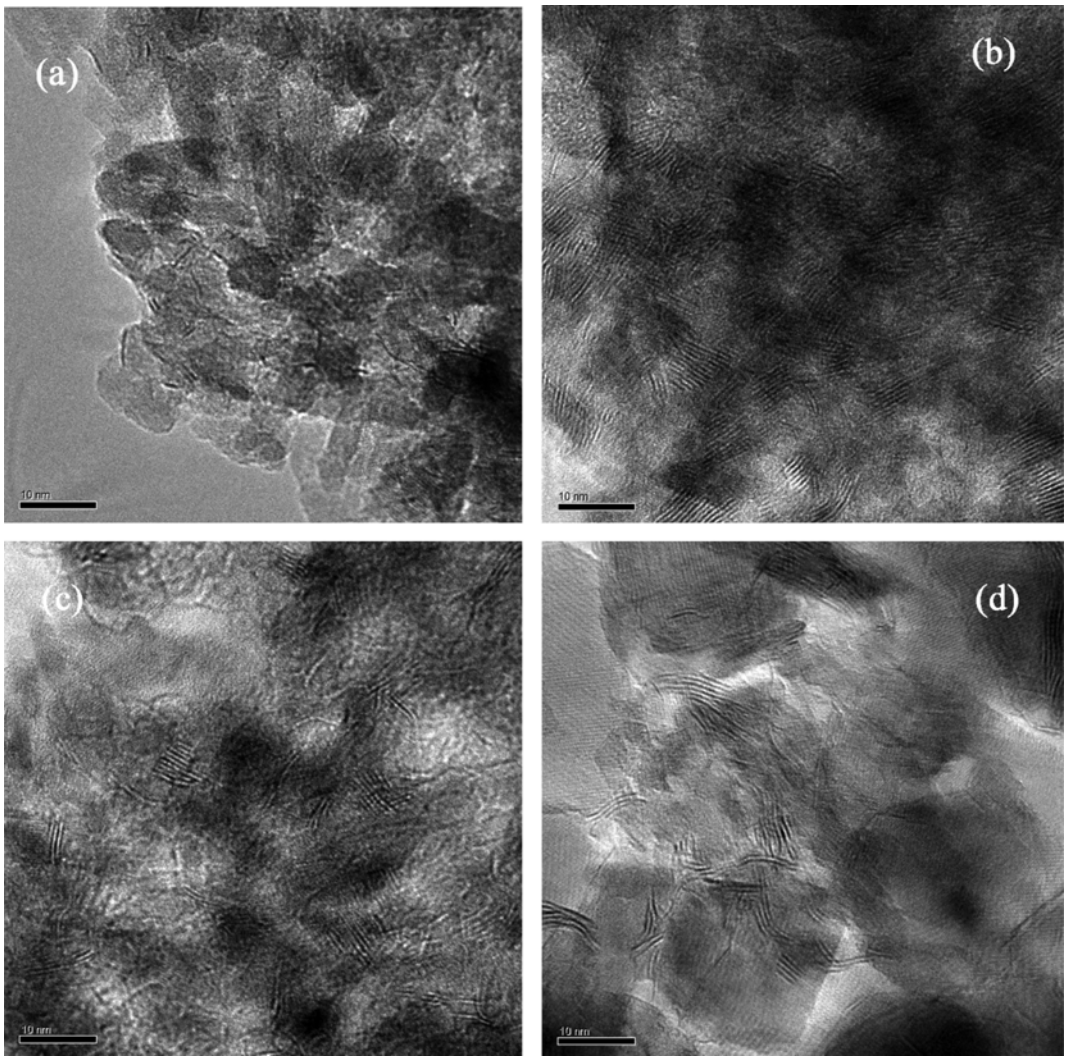

Fig. 2. HRTEM images of spent catalysts: (a) Mo/Al_2O_3, (b) MoS3-dry, (c) MoS3-450, (d) MoS3-600.

higher than that of DMDS sulfided catalyst. Ammonium thiosulfate had positive influence on the thiophene conversion. For presulfided catalysts, the calcinations conditions had important impact on the initial and final catalytic activity. If calcinations were applied to catalysts before impregnating with sulfiding agent, hydrogen activation was easier. The stabilization duration was at the sequence of MoS3-600<MoS3-450<MoS3-dry. However, the final HDS activity was at the sequence of MoS3-600<MoS3-450<MoS3-dry.

2. HRTEM Observation

The dispersion and morphology of the spent catalysts were investigated by HRTEM. The side-view images of MoS_2 hexagonal base planes with 0.62 nm inter-plane distance are shown in Fig. 2. Mo/Al_2O_3 possesses single layer MoS_2 structures (Type I), while the presulfided catalysts show mainly double or multi-layer MoS_2 slabs (Type II) [28]. The mean width and stacking number of MoS_2 slabs are calculated by measuring over 400 MoS_2 slabs. The results are listed in Table 1. The mean width and stacking number of Mo/Al_2O_3 are only 2.4 nm and 1.1, respectively, much smaller than those of presulfided catalysts. The strong interaction between MoS_2 slabs with Al_2O_3 prevents the active crystallines to grow. The presulfided catalysts show similar mean width of MoS_2 slabs. This illustrates that the different preparations have less influence on the mean width,

Table 1. Analysis of sulfur and carbon content in spent catalysts

Catalysts	C contents (wt%)	Molar ratio of S^{2-}/Mo	MoS_2 particles	
			Ave. width (nm)	Ave. stacking No.
Spent Mo/Al_2O_3	0.2	1.7	2.4	1.1
Spent MoS3-dry	3.3	1.9	3.2	3.4
Spent MoS3-450	1.9	1.8	3.2	3.0
Spent MoS3-600	1.5	1.3	3.2	2.5

but the stacking number increased with the decrease of the treatment temperature applied to the Mo metals. This suggests that the presulfidation technology can effectively decreases the interaction of active phase with support. High treatment temperature to Mo metal increased the interaction between active metal and support.

3. Sulfur and Carbon Element Analysis

Using the sulfur chemical analysis, the S/Mo molar ratios of fresh MoS3-dry MoS3-450 and MoS3-600 are 2.9, 3.0 and 2.9, respectively. These are almost the same as those added, indicating no sulfur losses during the presulfiding process. The S^{2-}/Mo mole ratios of spent catalysts are listed in Table 1. The spent MoS3-dry and MoS3-450 had S^{2-}/Mo ratios of 1.9 and 1.8, respectively, close to the stoichiometric ratio of ideal MoS_2 crystal. This indicates a sufficient sulfidation. In contrast, the S^{2-}/Mo molar ratio of the spent MoS3-600 is only 1.3; this is due to high temperature calcinations leading to some of Mo ions into Al_2O_3 support and formation of $Al_2(MoO_4)_3$; this part of Mo is difficult to sulfide [29]. The DMDS sulfided Mo/Al_2O_3 has an S^{2-}/Mo molar ratio of 1.6, lower than the stoichiometric ratio of MoS_2. This is a result of the strong interaction of Mo with Al_2O_3, which inhibits the sulfidation of Mo ions. The carbon content decreased in the order of MoS3-dry>MoS3-450>MoS3-600> Mo/Al_2O_3. The presulfided catalysts contained higher amount of carbon than the parent catalyst. The carbon species might modify active phase or exist as coke [30].

4. BET Analysis

To investigate the influence of ammonium thiosulfate on the physical properties of catalyst, BET analysis was carried out on the fresh and the spent catalysts, as well as support (Table 2). For the fresh MoS3-dry and MoS3-450, the surface areas and pore volumes decreased apparently after being impregnated with Mo metal and ammonium thiosulfate, although the pore diameter was not apparently changed. The decreased degree of surface area and pore volume is much larger for the MoS3-600, accompanied with the increase in the average pore size. This is due to collapse of pores at high calcination temperature. After HDS reaction, the surface area of Mo/Al_2O_3 was not changed, but pore volume and average pore size dropped slightly. In contrast, the surface areas of MoS3-dry and MoS3-450 had recovered to the level of the parent catalyst, while the pore volume and the average pore diameter were slightly smaller than that of Mo/Al_2O_3. This indicates that the presulfidation did not change the support porosity. The decrease in the pore volume and the average pore size may be due to the block of pores by carbon species. Nevertheless, the surface area and the pore volume of MoS3-600 were much less than those of Mo/Al_2O_3. The average pore size is almost twice as much as that of Mo/Al_2O_3. This evidenced the collapse of the support.

Table 2. Textural properties of fresh and spent catalysts

Catalysts	Average pore diameter (nm)	Pore volume (cm^3/g cat)	BET surface area (m^2/g cat)
γ-Al_2O_3	8.0	0.46	230
Fresh Mo/Al_2O_3	9.1	0.40	176
Fresh MoS3-dry	8.1	0.24	120
Fresh MoS3-450	9.8	0.24	116
Fresh MoS3-600	26.2	0.14	21
Spent Mo/Al_2O_3	8.3	0.37	178
Spent MoS3-dry	7.5	0.32	170
Spent MoS3-450	8.2	0.33	164
Spent MoS3-600	16.9	0.24	56

5. TG-MS Test

Fig. 3 shows the TG-DTG profiles over different samples. Three weight loss regions were observed below 250 °C for $(NH_4)_2S_2O_3/Al_2O_3$ (Fig. 3(a)). SO_2 and a small amount of SO_3 was detected by MS between 150 and 350 °C. The ammonium thiosulfate is an unstable compound, which decomposes at about 150 °C in air to ammonium sulfurous acid, sulfur, ammonium and water, etc. The weight loss below 100 °C is ascribed to the desorption of absorbed water, while loss in the range of 100-250 °C is attributed to the decomposition of ammonium thiosulfate.

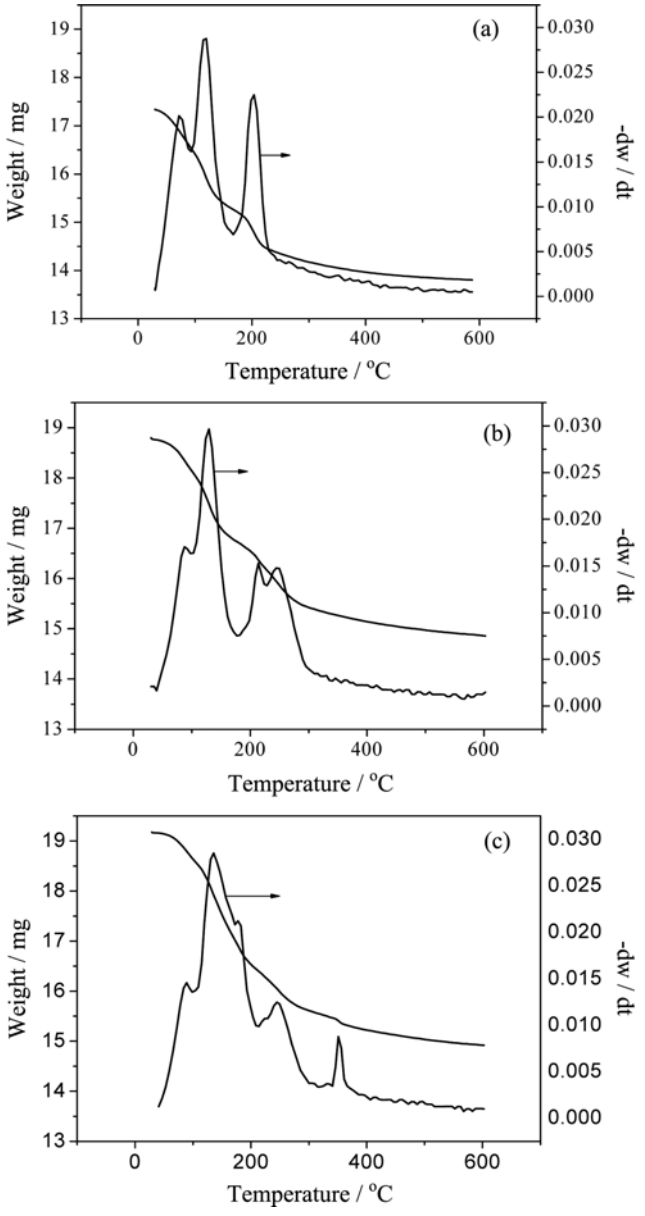

Fig. 3. TG-DTG spectra of samples: (a) $(NH_4)_2S_2O_3/Al_2O_3$ in 20% O_2-80% Ar; (b) $(NH_4)_2S_2O_3/Al_2O_3$ in 10% H_2-90% Ar; (c) MoS3-dry in 10% H_2-90% Ar.

Table 3. XPS analysis of catalysts after H_2 activation and after HDS reaction

Catalyst	Mo3$d_{5/2}$ (eV)	Fraction (%)	S 2$p_{3/2}$ (eV)	Fraction (%)	S^{6+}/S^{2-}	S^{2-}/Mo
MoS3-dry after activation	227.9 (1.6)	75	161.4 (1.4)	81	0.2	0.7
	229.3 (1.3)	12	167.2 (3.0)	19		
	231.8 (2.1)	13				
MoS3-450 after activation	228.5 (2.3)	61	161.7 (2.5)	75	0.3	0.9
	231.0 (1.2)	8	169.0 (2.1)	25		
	232.6 (2.3)	31				
MoS3-600 after activation	228.5 (1.9)	55	161.6 (2.7)	77	0.2	0.9
	230.9 (1.3)	20	169.0 (2.4)	23		
	232.6 (1.1)	25				
MoS3-dry after HDS	228.4 (1.5)	74	161.5 (1.9)	76	0.1	1.7
	230.5 (2.9)	9	168.5 (2.1)	23		
	232.2 (1.9)	17				
MoS3-450 after HDS	228.5 (1.7)	71	161.4 (1.8)	84	0.2	1.7
	230.7 (2.0)	15	168.2 (2.1)	16		
	232.2 (1.6)	14				
MoS3-600 after HDS	228.6 (1.9)	63	161.2 (1.7)	81	0.2	1.3
	230.0 (2.5)	13	168.7 (1.7)	19		
	231.9 (2.1)	24				
Mo/Al_2O_3 after HDS	228.4 (1.9)	71	161.2 (1.6)	100	0.0	1.6
	230.0 (1.5)	15				
	231.7 (2.0)	14				

*The full widths at half maximum are given in parentheses

Four weight loss regions were observed for $(NH_4)_2S_2O_3/Al_2O_3$ heated in reductive atmosphere (Fig. 3(b)). The first three regions are similar to those observed in air atmosphere. Between 200 and 250 °C, SO_2 and H_2S was observed by MS. This suggests that the fourth weight loss region might be attributed to reductive decomposition of resides formed through the decomposition of $(NH_4)_2S_2O_3$ at lower temperature.

The different $(NH_4)_2S_2O_3$ presulfided catalysts showed similar TG-DTG profiles; thus as an example the TG/DTG curves of MoS3-dry in reductive gas atmosphere were shown. Clearly, there are five weight loss regions. The regions corresponding to DTG peaks at 90 and 135 °C are due to desorption of water and initial decomposition of $(NH_4)_2S_2O_3$, while ones around 180 and 250 °C can be attributed to the reductive decomposition of $(NH_4)_2S_2O_3$. For the weight loss larger than 300 °C, MS measurement shows that a large amount of hydrogen was consumed although no sulfur species can be detected around this temperature. According to ref. [31], during sulfidation of Mo-based catalysts, the Mo^{6+} ions are reduced to Mo^{4+} through the Mo^{5+} intermediates. The highest reduction rate was observed between 300 to 400 °C. Therefore, the weight loss larger than 300 °C could be ascribed to the reduction of Mo. From above results, we can conclude that the sulfidation of Mo mainly takes place between 130 and 300 °C, and reduction mainly occurs between 300 and 400 °C.

6. XPS Characterization

To investigate the change in valence and coordination of Mo and S ions during hydrogen activation and thiophene HDS reaction, XPS measurements were conducted over the catalysts after activation and HDS reaction, respectively. The Mo $3d_{5/2}$ with BE around 232 eV represents the oxidized Mo^{6+} species, the Mo $3d_{5/2}$ of sulfided Mo^{4+} appears at about 228 eV, and Mo $3d_{5/2}$ at 230 eV is attributed to the Mo^{5+} intermediate ions of oxysulfide [32]. For the S 2p spectra, the BEs at about 162 and 168 eV is attributed to S^{2-} ligands and S^{6+} species, respectively [33]. The envelopes of Mo and S ions were deconvoluted by XPSPEAK 4.1 software and the relative content was calculated by the sensitive factors provided by instrument provider.

The XPS results are listed in Table 3. The S^{2-}/Mo molar ratios of presulfided catalysts after activation and HDS reaction show large differences. The relative content of Mo^{6+}, Mo^{5+} and Mo^{4+} is almost the same before and after HDS reaction for MoS3-dry, but its S^{2-}/Mo ratio increases from 0.7 to 1.7. During activation the S^{2-} ligands may be stripped by hydrogen from the active surface [34]. This would result in a low S^{2-} content on the surface of the activated catalyst. However, the stripped sulfur can be supplemented by the sulfur of thiophene during HDS reaction. This also held true for MoS3-450 and MoS3-600, although the relative content of Mo^{4+} slightly increased during HDS reaction. This shows that besides the sulfur supplement, the reductive sulfidation of Mo also occurs during HDS reaction for these two presulfided catalysts. The results illustrate that the sulfidation for a presulfided catalyst can be well achieved through both ammonium thiosulfate presulfidation and HDS reaction.

Although the atomic ratio of S^{6+} to S^{2-} in ammonium thiosulfate is 1, the relative content of S^{6+} is much smaller than that of S^{2-} after activation. This discrepancy suggests that much more of S^{6+} ions are released in the form of SO_2, as shown by TG-MS. The remained sulfate species may primarily come from the $Al_2(SO_4)_3 \cdot 5H_2O$, which can be detected in fresh presulfided catalyst by XRD [25].

7. NH_3-TPD Acidity Measurement

Fig. 4 shows the NH_3-TPD profiles of spent catalysts. The acid sites have been classified on the basis of an arbitrary range: weak

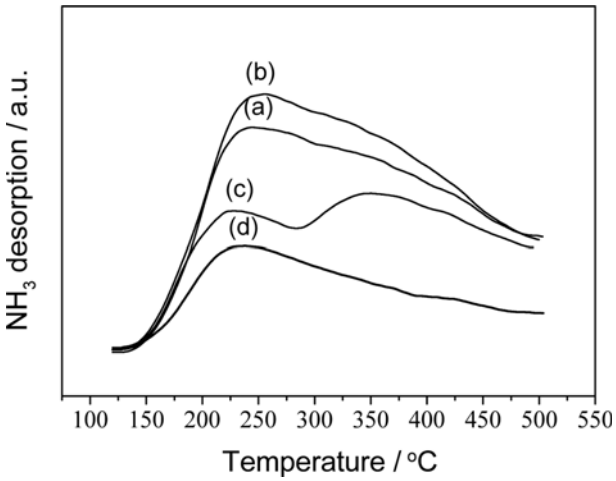

Fig. 4. NH_3-TPD curves of spent catalysts: (a) Mo/Al_2O_3, (b) MoS3-dry, (c) MoS3-450, (d) MoS3-600.

(120-220 °C), medium (220-350 °C), and strong (350-550 °C) [35]. Table 4 compiles the number of weak, medium and strong sites obtained by such classification. As seen in this table, MoS3-450 shows two types (weak and strong) of acid sites, while others possess the weak, medium and strong acid sites. Considering the total number of acid sites, the observed trend is: MoS3-dry>Mo/Al_2O_3>MoS3-450>MoS3-600. Although the sulfate groups are present on the presulfided catalysts, the acidity does not increase. This suggests that the combination of sulfate groups with aluminum ions inhibited the formation of new acidic centers.

The acidities of the presulfided catalysts are significantly different. Because MoS_2 shows almost no acidity, the acidity of samples mainly comes from the acidic hydroxyl group of alumina support. The low acidity of MoS3-600 is due to the condensation of hydroxyl groups of support caused by calcination at high temperature. In the Mo/Al_2O_3 catalyst, MoS_2 interacts strongly with basic hydroxyl groups of Al_2O_3 support [36], and thus the acidic sites on the support surface are kept almost intact. In contrast, for the presulfided catalysts, the sulfate species may compete with MoS_2 to interact with basic hydroxyl group. This would cause part of MoS_2 to interact with mediate acidic hydroxyl group, weakening the acidity of support. As a result, MoS3-450 shows lower acidity than Mo/Al_2O_3. As for MoS3-dry, no calcination was applied to the Mo precursor; thus, the surface hydroxyl groups were reserved, exhibiting slightly higher acidity.

DISCUSSION

In the presulfided catalyst, parts of the metal oxides are transformed into oxysulfides or sulfides [37]. Moulijn et al. [11] reported that extensive O-S exchange occurs below 200 °C between MoO_3 and H_2S when H_2S is used to sulfide MoO_3/Al_2O_3. De Boer et al. [12] found through EXAFS that even at room temperature the O is also considerably exchanged with S in Mo/SiO_2.

In this experiment, the catalysts after impregnation with $(NH_4)_2S_2O_3$ were heat-treated at 90 °C for 2 h in air. The XRD results of our previous experiment evidenced the formation of $Al_2(SO_4)_3 \cdot 5H_2O$ phase [25,38]. It was proposed that a part of $(NH_4)_2S_2O_3$ is transformed into $(NH_4)_2SO_4$ through O-S exchange with Mo oxides, then the $(NH_4)_2SO_4$ intermediate reacts with Al_2O_3 to form $Al_2(SO_4)_3 \cdot 5H_2O$. The XRD also showed that the other $(NH_4)_2S_2O_3$ were still reserved on the presulfided catalyst. During the hydrogen activation, this part of $(NH_4)_2S_2O_3$ decomposed and sulfided the Mo specie, and the Mo^{+6} ions were simultaneously reduced to Mo^{+4} ions. The TG-MS results show that the $(NH_4)_2S_2O_3$ decompose and produce H_2S and SO_2, etc., between 130 and 300 °C, The H_2S can react with Mo oxides or oxysulfides. The reductive reaction of Mo^{+6} occurs mainly at 300-400 °C. The XPS results shows that after activation the S^{2-}/Mo molar ratio in the presufided catalysts is much smaller than that (1.5) of fresh catalysts. This indicates that the S^{6+} ions in ammonium thiosulfate might not take part in the sulfidation of Mo ions.

By the temperature programmed sulfidation (TPS), Scheffer et al. [39,40] observed the H_2S release at about 225 °C. They proposed that the breaking of Mo-S bond of MoS_3 intermediate produces elemental sulfur, which is then reduced to H_2S. De Boer et al. [12] found in MoO_3/SiO_2 catalyst that increasing the temperature to 150 °C leads to the formation of MoS_3 analogies, which are transformed into MoS_2 between 250 and 300 °C. Payen et al. [14] could identify different proportions of intermediates, such as oxysulfide and MoS_3 during the sulfidation of MoO_3/Al_2O_3 by in situ Raman technology. However, de Jong et al. [41] could not find evidence for the formation of elemental sulfur when studying $MoO_3/SiO_2/Si$ catalyst. They suggested that at low temperature MoO_2 or H_xMoO_3 species are included in the interior, while Mo^{4+} oxysulfides are formed on the surface.

In this study, the mole ratios of S^{6+}/S^{2-} of presulfided catalysts were found to drop from 1.0 to 0.2-0.3 after hydrogen activation. The TG-MS experiment showed the SO_2 release under air or reductive atmosphere. Thus it is postulated that the initial decomposition of ammonium thiosulfate produced the elemental sulfur and SO_2. Then the elemental sulfur intermediate was reduced to H_2S, as shown in Eq. (1) and (2). And the $(NH_4)_2SO_3$ intermediate continually decomposed to release NH_3, H_2O and SO_2.

$$(NH_4)_2S_2O_3 \rightarrow (NH_4)_2SO_3 + S \quad (1)$$

Table 4. Surface acidity of spent catalysts measured by TPD-NH_3

Catalysts	Total acidity ($\mu molNH_3/g$)	Dispersion of acidity ($\mu molNH_3/g$) (%)		
		Weak	Mediate	Strong
Spent Mo/Al_2O_3	360	90 (25%)	137 (38%)	133 (37%)
Spent MoS3-dry	417	163 (39%)	109 (26%)	144 (35%)
Spent MoS3-450	230	76 (33%)	0	154 (67%)
Spent MoS3-600	156	63 (40%)	80 (51%)	13 (9%)

$$S+H_2 \rightarrow H_2S \quad (2)$$

By comparing the sulfiding intermediates in $MoO_3/SiO_2/Si(100)$ with the $(NH_4)_2[Mo_3S_{13}]\cdot H_2O$ cluster, Muijsers et al. [42] thought that the sulfidation goes through a Mo^{5+} intermediate species ($MoOS_{1.5}$). Guichard et al. [43] found the Mo^{5+} oxysulfides in the sulfided Mo catalysts. The XPS results of the presulfided catalysts showed the existence of Mo^{5+} ions, suggesting the formation of Mo oxysulfides.

We deduced that (a) the Mo^{6+} oxysulfides intermediate are formed by O-S exchange during presulfidation and activation (as shown in Eqs. (3) and (4)), (b) the Mo^{5+} oxysulfides are formed in activation (Eq. (5)), (c) elemental sulfur intermediate originates from the decomposition of sulfiding agent, and (d) the MoS_3 intermediate may not form because of the limited supplication of H_2S in activation.

$$y(NH_4)_2S_2O_3+MoO_3=y(NH_4)_2SO_4+MoO_{3-y}S_y \quad (3)$$

$$MoO_3+yH_2S=MoO_{3-y}S_y+xH_2O \quad (4)$$

$$MoO_{3-y}S_y+H_2=MoOS_{1.5}+(2-y)H_2O+(y-1.5)H_2S \quad (5)$$

The HRTEM shows that the active phases of presulfided catalysts have multi-layer type II structures, and the DMDS sulfided Mo/Al_2O_3 shows mainly single MoS_2 slabs. Candia et al. [44] reported that in an increase in the sulfiding temperature from 400 to 600 °C, the structure of the active phase of $CoMo/Al_2O_3$ catalysts transformed from type I to type II. The type I active phase interacts strongly with alumina, forming Mo-O-Al linkage, whereas the type II structure exhibits only a weak van der Waals interaction with support. Catalysts with type II active phases show higher intrinsic activities [45]. The transformation of type I to type II can be made possible by addition of ligands, or use of support with weak interaction, such as carbon [46-51]. Prins et al. [52,53] found that passivation by air led to formation of sulfate species on sulfided $Co(Ni)Mo/Al_2O_3$ catalyst and induced the structure transformed from type I to type II Co(Ni)-Mo-S active phase.

The XPS shows that the S^{6+} ions were present on the surface of the presulfided catalyst after activation and HDS reaction (Table 3). $Al_2(SO_4)_3\cdot 5H_2O$ phase in the support should represent these sulfate species. It is deduced that the basic Al-OH group reacts with acidic sulfate species to form the $Al_2(SO_4)_3$. This resulted in the decrease of interaction of Mo with Al_2O_3, and the formation of Type II MoS_2 structures, as illustrated in Scheme 1.

The effect of sulfate species on Mo/Al_2O_3 catalysts is comparable to that of phosphate. The phosphate has been extensively applied in refineries to improve HDS catalysts. After introduction of phosphate, the $AlPO_4$ formed on the surface of alumina support decreases the interaction of support with oxide precursors [54]. HRTEM images showed that addition of phosphate increases the stacking number and width of MoS_2 crystallites in Mo/Al_2O_3 and $CoMo/Al_2O_3$ catalysts [55]. The enhancement in stacking suggests the formation of Type II Co-Mo-S structures. Our results show that the sulfate species in $(NH_4)_2S_2O_3$ presulfided catalysts plays a role similar to that phosphate does.

After hydrogen activation, the S^{2-}/Mo ratios of presulfided catalysts are smaller than 1.0 (Table 3). TG-MS measurement shows that the temperature for decomposition of $(NH_4)_2S_2O_3$ into SO_2 and H_2S is between 130 and 300 °C. However, only over 300 °C, sulfided Mo-based catalyst can catalyze the SO_2 gas reduced into elemental sulfur and H_2S under hydrogen atmosphere, the yield of H_2S increases with increasing temperature [56]. The SO_2 originating from decomposition of $(NH_4)_2S_2O_3$ cannot be reduced into H_2S in this experiment. Owing to the shortage of H_2S, the presulfided catalysts cannot be effectively sulfided during activation. However, after HDS reaction, the sulfiding degree has enhanced apparently. The S^{2-}/Mo of MoS3-dry and MoS3-450 have increased over 1.7. MoS3-600, owing to calcinations at the high temperature, shows less S^{2-}/Mo. We determined that during thiophene HDS a supplementary sulfidation occurs, namely, the sulfur removed from thiophene remains on the MoS_x active phases; thus the Mo is sulfided continually by thiophene. Meanwhile, some oxysulfide can be further sulfided to MoS_2, as evidenced by XPS. The total sulfidation process is illustrated in Scheme 2. After the supplementary sulfidation, the $(NH_4)_2S_2O_3$ presulfided catalysts show much better HDS performance than Mo/Al_2O_3 sulfided by DMDS, as shown in Fig. 1.

From the above results and analyses, it could be concluded that during presulfidation and activation the S^{2-} ions in $(NH_4)_2S_2O_3$ sulfide the Mo ions, while S^{6+} species weaken the interaction of Mo with Al_2O_3 support and enhance the sulfiding degree. Their synergetic effect results in the formation of Type II MoS_2 active phases. On the other hand, the $(NH_4)_2S_2O_3$ presulfided catalysts showed similar or lower acidity compared to the catalyst sulfided by DMDS; this excludes the possibility that the HDS activity is facilitated by the crack of sulfur-containing compound. XPS results show that the MoS3-dry and MoS3-450 catalysts have a Mo^{4+} relative content similar to the DMDS sulfided catalyst, and MoS3-600 has lower Mo^{4+} relative content, excluding the enhancement in catalytic activ-

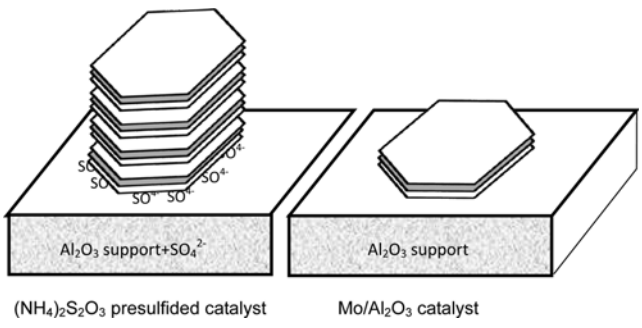

Scheme 1. Active phase and support models of $(NH_4)_2S_2O_3$ presulfided and DMDS sulfided Mo/Al_2O_3 catalysts.

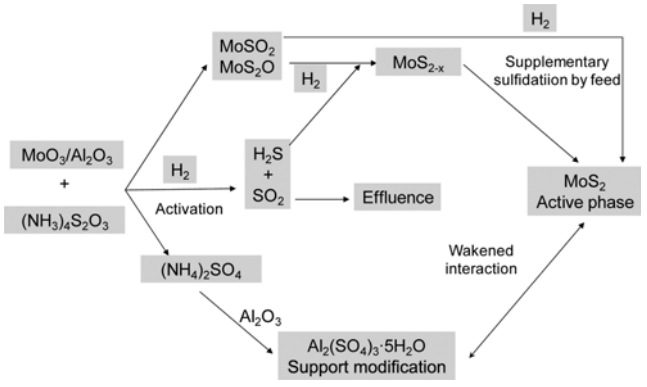

Scheme 2. Schematic presulfidation and activation mechanism of Mo/Al_2O_3 catalyst presufided by $(NH_4)_2S_2O_3$.

ity by higher content of MoS_2. Although the high calcination temperature used for MoS3-600 causes low sulfidation degree and Mo^{4+} relative content, this catalyst still showed higher HDS activity than DMDS sulfided Mo/Al_2O_3. This suggests that the formation of Type II MoS_2 is the main reason for the high catalytic activities of $(NH_4)_2S_2O_3$ presulfided catalysts and the sulfiding degree has less meaning for the HDS activity.

CONCLUSIONS

During impregnation of Mo/Al_2O_3 with $(NH_4)_2S_2O_3$, the Mo is partly sulfided through the O-S exchange; the intermediate of $(NH_4)_2SO_4$ reacts with Al_2O_3 support to form $Al_2(SO_4)_3$, which weakens the interaction of active metal with support. The Mo species are further sulfided by $(NH_4)_2S_2O_3$ and reduced by hydrogen in the activation process, and the multi-layer Type II MoS_2 active phases are formed. The insufficiency of S^{2-} ligands in presulfied catalysts resulted in a molar ratio of S^{2-}/Mo lower than 1.0 after activation process. In HDS reaction, the S^{2-}/Mo molar ratio was markedly enhanced through a supplementary sulfidation, being close to the ideal stoichiometric ratio of 2. The $(NH_4)_2S_2O_3$ presulfided catalysts show higher thiophene HDS activities than DMDS-sulfided Mo/Al_2O_3 catalyst. This is due to the formation of intrinsically highly active Type II phases in former catalyst. An increase in the sulfiding degree may also have a positive effect on the HDS activity. The different sulfur atoms in $(NH_4)_2S_2O_3$ play different roles; the S^{2-} sulfides the Mo ion, while the S^{6+} modifies the support. The cooperation of these two types of S ions makes the $(NH_4)_2S_2O_3$ presulfided catalysts exhibit excellent HDS activities.

ACKNOWLEDGEMENTS

We gratefully acknowledge the financial supports from National Basic Research Program of China (973) (2006CB202504).

REFERENCES

1. C. Song, *Catal. Today*, **86**, 211 (2003).
2. N. Frizi, P. Blanchard, E. Payen, P. Baranek, M. Rebeilleau, C. Dupuy and J. P. Dath, *Catal. Today*, **130**, 272 (2008).
3. K. L. Kim and K. S. Choi, *Korean J. Chem Eng*., **5**, 177 (1988).
4. S. Z. Abghari, S. Shokri, B. Baloochi, M. A. Marvast, S. Ghanizadeh and A. Behroozi, *Korean J. Chem. Eng*., **28**, 93 (2011).
5. J. G. Welch, P. Poyer and R. F. Skelly, *Oil Gas J*., **92**, 56 (1994).
6. P. Dufresne, N. Brahma and S. R. Muff, US Patent, 5,985,787 (1993).
7. M. de Wind, J. J. L. Heinerman, S. L. Lee and F. L. Plantenga, *Oil Gas J*., **90**, 49 (1992).
8. W. Qian, S. Yamada, A. Ishihara, M. Ichinoseki and T. Kabe, *Sekiyu Gakkaishi*, **44**, 225 (2001).
9. H. Ge, X. Li, Z. Qin, F. Liang and J. Wang, *Korean J. Chem. Eng*., **26**, 576 (2009).
10. F. E. Massoth, *J. Catal*., **36**, 164 (1975).
11. P. Arnold, J. A. M. van den Heijkant, G. D. de Bok and J. A. Moulijn, *J. Catal*., **92**, 35 (1985).
12. M. de Boer, A. J. van Dillen, D. C. Koningsberger and J. W. Geus, *J. Appl. Phys*., **32**, 460 (1993).
13. T. H. Weber, J. C. Muijsers, J. H. M. C. van Wolput, C. P. J. Verhagen and J. W. Niemantsverdriet, *J. Phys. Chem*., **100**, 14144 (1996).
14. E. Payen, S. Kasztelan, S. Houssenbay, R. Szymanski and J. Grimblot, *J. Phys. Chem*., **93**, 6501 (1989).
15. R. Prada Silvy, P. Grange and B. Delmon, *Stud. Surf. Sci. Catal*., **53**, 233 (1989).
16. A. M. de Jong, H. J. Borg, L. J. van Ijzendoorn, V. G. F. M. Soudant, V. H. J. de Beer, J. A. R. van Veen and J. W. Niemantsverdriet, *J. Phys. Chem*., **97**, 6477 (1993).
17. J. Ramírez and F. Sánchez-Minero, *Catal. Today*, **130**, 267 (2008).
18. E. J. M. Hensen, V. H. J. de Beer, J. A. R. van Veen and R. A. van Santen, *Catal. Lett*., **84**, 59 (2002).
19. Y. Okamoto, A. Kato, Usman, N. Rinaldi, T. Fujikawa, H. Koshika, I. Hiromitsu and T. Kubota, *J. Catal*., **265**, 216 (2009).
20. A. I. Dugulan, E. J. M. Hensen and J. A. R. van Veen, *Catal. Today*, **130**, 126 (2008).
21. B. Hinnemann, J. K. Nøskov and H. Topsøe, *J. Phys. Chem. B*, **109**, 2245 (2005).
22. L. S. Byskov, J. K. Nørskov, B. S. Clausen and H. Topsøe, *J. Catal*., **187**, 109 (1999).
23. P. Raybaud, J. Hafner, G. Kresse, S. Kasztelan and H. Toulhoat, *J. Catal*., **189**, 129 (2000).
24. H. Ge, X. Li, Z. Qin, Z. Lü and J. Wang, *Catal. Commun*., **9**, 2578 (2008).
25. H. Ge, X. Li, W. Fan, Z. Qin, Z. Lü and J. Wang, Chin. *J. Catal*., **30**, 111 (2009).
26. N. Rueda, R. Bacaud and M. Vrinat, *J. Catal*., **169**, 404 (1997).
27. H. Topsøe, B. Hinnemann, J. K. Nørskov, J. V. Lauritsen, F. Besenbacher, P. L. Hansen, G. Hytoft, R. G. Egeberg and K. G. Knudsen, *Catal. Today*, **12**, 107 (2005).
28. G. Plazenet, E. Payen, J. Lynch and B. Rebours, *J. Phy. Chem. B*, **106**, 7013 (2002).
29. R. Berhault, A. Mehta, A. C. Pavel, J. Z. Yang, L. Rendon, M. J. Yácaman, L. C. Araiza, A. D. Moller and R. R. Chianelli, *J. Catal*., **198**, 9 (2001).
30. S. Texier, G. Berhault, G. Pérot and F. Diehl, *Appl. Catal. A*, **293**, 105 (2005).
31. V. La Parola, G. Deganello and A. M. Venezia, *Appl. Catal. A*, **260**, 237 (2004).
32. H. Y. Shang, C. G. Liu, R. Y. Zhao, M. B. Wu and F. Wei, *Chin. J. Chem*., **22**, 1250 (2004).
33. J. F. Paul, S. Cristol and E. Payen, *Catal. Today*, **130**, 139 (2008).
34. D. Ferdous, A. K. Dalai and J. Adjaye, *Appl. Catal. A*, **260**, 137 (2004).
35. N. Y. Topsøe and H. Topsøe, *J. Catal*., **139**, 631 (1993).
36. S. Blashka, G. Bond and D. Ward, *Oil Gas J*., **96**, 36 (1998).
37. H. Ge, X. Li, J. Wang, Z. Lü, Z. Qin and L. Zhou, *J. Fuel Chem. Technol*., **37**, 199 (2009).
38. B. Scheffer, P. Arnoldy and J. A. Moulijn, *J. Catal*., **112**, 516 (1988).
39. B. Scheffer, E. M. van Oers, P. Arnoldy, V. J. H. de Beer and J. A. Moulijn, *Appl. Catal*., **25**, 303 (1986).
40. A. M. de Jong, H. J. Borg, L. J. van Ijzendoorn, V. G. F. M. Soudant, V. H. J. de Beer, J. A. R. van Veen and J. W. Niemantsverdriet, *J. Phys. Chem*., **97**, 6477 (1993).
41. J. C. Muijsers, T. H. Weber, R. M. van Hardeveld, H. W. Zandbergen and J. W. Niemantsverdriet, *J. Catal*., **157**, 698 (1995).
42. B. Guichard, M. Roy-Augerger, E. Devers, C. Legens and P. Ray-

baud, *Catal. Today*, **130**, 97 (2008).
43. R. Candia, O. Sørensen, J. Villadsen, N. Y. Topsøe, B. S. Clausen and H. Topsøe, *Bull. Soc. Chim. Belg*., **93**, 763 (1984).
44. H. Topsøe and B. S. Clausen, *Appl. Catal*., **25**, 273 (1986).
45. M. Sun, D. Nicosia and R. Prins, *Catal. Today*, **86**, 173 (2003).
46. L. Medici and R. Prins, *J. Catal*., **163**, 28 (1996).
47. T. Fujikawa, H. Kimura, K. Kiriyama and K. Hagiwara, *Catal. Today*, **111**, 188 (2006).
48. T. F. Hayden, J. A. Dumesic, R. D. Sherwood and R. T. K. Baker, *J. Catal*., **105**, 299 (1987).
49. J. P. R. Vissers, B. Scheffer, J. H. J. de Beer, J. A. Moulijn and R. Prins, *J. Catal*., **105**, 277 (1987).
50. J. A. R. van Veen, E. Gerkema, A. M. van der Kraan and A. Knoester, *Chem. Commun*., 1684 (1987).
51. S. P. A. Louwers, M. W. J. Crajé, A. M. van der Kraan, C. Geantet and R. Prins, *J. Catal*., **144**, 579 (1993).
52. V. M. Browne, S. P. A. Louwers and R. Prins, *Catal. Today*, **10**, 345 (1991).
53. Usman, T. Yamamoto, T. Kubota and Y. Okamoto, *Appl. Catal*., **328**, 219 (2007).
54. S. Yamada, W. Qian, A. Ishihara, G. Wang. L. Li and T. Kabe, *Sekiyu Gakkaishi*, **44**, 217 (2001).
55. C. L. Chen, C. H. Wang and H. S. Weng, *Chemosphere*, **56**, 425 (2004).